Dynamics of Certain Nonconformal Degree-Two Maps of the Plane

Ben Bielefeld, Scott Sutherland, Folkert Tangerman and J. J. P. Veerman

CONTENTS

We consider the rational maps given by $z \mapsto |z|^{2\alpha-2}z^2 + c$, for z and c complex and $\alpha > \frac{1}{2}$ fixed and real. The case $\alpha = 1$ corresponds to quadratic polynomials: some of the well-known results for this conformal case still hold for α near 1, while others break down. Among the differences between the two cases are the possibility, for $\alpha \neq 1$, of periodic attractors that do not attract the critical point, and the fact that for $\alpha < 1$ the Julia set is smooth for an open set of values of c. Numerical evidence suggests that the analogue of the Mandelbrot set for this family is connected, but not locally connected if $\alpha \neq 1$.

INTRODUCTION

We consider a family of maps that are similar to quadratic maps in being degree-two branched covers of the Riemann sphere, but that are not in general conformal. Namely, for $\alpha > \frac{1}{2}$ real and fixed, we study maps f_c given in polar coordinates by

$$f_c(re^{i\theta}) = r^{2\alpha}e^{2i\theta} + c.$$

For $\alpha = 1$, this is the usual quadratic family ($z \mapsto z^2 + c$), which has been extensively studied and is fairly well understood. For α different from one, f_c is only quasiconformal, and very different behavior can occur, although there are many strong similarities to the conformal case. It is our goal to determine which results for the quadratic family can be generalized to maps that are topologically similar (and when α is close to 1, close to quadratic), and where such results break down.

In the quadratic family, the orbit of the critical point completely determines the dynamics. This is not the case for the maps f_c: for example, we have found periodic attractors that do not attract

1058-6458/96 \$0.50 per page

the critical point. For certain parameter values, the dynamics is dominated by two-dimensional real behavior: periodic saddle points, invariant circles, and so on.

Another striking difference with the quadratic family is the existence of smooth Julia sets. In the conformal case, the only smooth Julia sets are the segment $[-2,2]$ (for the map $z \mapsto z^2-2$) and the unit circle (for the map $z \mapsto z^2$). The corresponding Julia sets for f_c are also smooth, but there are more: we use structural stability techniques to show that for any $\alpha < 1$, the Julia set is C^k-smooth for all c-values sufficiently near 0.

We also study the connectedness locus (the analogue of the Mandelbrot set), and the bifurcations that occur in the c-plane. Numerical evidence suggests strongly that the connectedness locus is always connected, and never locally connected for $\alpha \neq 1$. Furthermore, the bifurcations that occur as the parameter c varies are considerably more complicated than those in the conformal case, although there are many similarities. We discuss these issues at some length in Sections 4 and 5.

1. DEFINITIONS AND ELEMENTARY RESULTS

For $\alpha > 0$, consider the map Q_α given by

$$Q_\alpha(re^{i\theta}) = r^\alpha e^{i\theta}$$

in polar coordinates, or, equivalently, by

$$Q_\alpha(z) = z^{(\alpha+1)/2}\bar{z}^{(\alpha-1)/2}$$

in $(z,\bar{z})$ coordinates, for appropriate branches of the powers. The family $\{Q_\alpha\}$ is a one-parameter group: $Q_\alpha \circ Q_\beta = Q_{\alpha\beta}$. Each Q_α is a quasiconformal homeomorphism of the Riemann sphere of constant dilatation $\max(\alpha,\alpha^{-1})$. (See [Lehto 1987] for the definition of a quasiconformal map.) The proof is a straightforward computation: the dilatation is

$$\frac{|\partial Q_\alpha| + |\bar\partial Q_\alpha|}{|\partial Q_\alpha| - |\bar\partial Q_\alpha|} = \frac{\alpha+1+|\alpha-1|}{\alpha+1-|\alpha-1|} = \max(\alpha,\alpha^{-1}),$$

where $\partial = \partial/\partial z$ and $\bar\partial = \partial/\partial\bar z$.

Denote by P_c the quadratic map on $\mathbb{C}$ given by $P_c(z) = z^2 + c$, and let $f_{\alpha,c} = P_c \circ Q_\alpha$. Thus

$$f_{\alpha,c}(z) = \begin{cases} |z|^{2\alpha-2}z^2 + c & \text{or} \\ z^{\alpha+1}\bar z^{\alpha-1} + c & \text{in } (z,\bar z)\text{-coordinates or} \\ r^{2\alpha}e^{i2\theta} + c & \text{in polar coordinates.} \end{cases}$$

For any $\alpha > 0$ and any $c \in \mathbb{C}$, the map $f_{\alpha,c}$ is a branched cover of $\mathbb{C}$ with a single branch point, the origin, where the map is ramified of degree two. It extends to the Riemann sphere with a branch point at ∞ of degree two. Throughout this paper we always assume that $\alpha > \frac{1}{2}$. This guarantees that the dynamics near infinity is always the same: the point ∞ is attracting. Moreover, when $\alpha > \frac{1}{2}$, each $f_{\alpha,c}$ is at least once differentiable everywhere.

Define the *filled-in Julia set* $K(\alpha,c)$ of $f_{\alpha,c}$ as the set of points whose orbits under $f_{\alpha,c}$ do not accumulate at ∞ (see Figure 1 for examples). Define the *Julia set* $J(\alpha,c)$ as the the set of points that have no neighborhood in which the iterates of $f_{\alpha,c}$ form an equicontinuous family in the spherical metric. Because $f_{\alpha,c}$ is an open map, the Julia set can be split up into two completely invariant (that is, forward and backward invariant) subsets $\partial K(\alpha,c)$ and $\Delta(\alpha,c) = J(\alpha,c) \setminus \partial K(\alpha,c)$. When $\alpha = 1$ the set $\Delta(\alpha,c)$ is empty, but in general it is nonempty. For instance, $\Delta(\alpha,c)$ may contain stable manifolds of periodic saddle points.

Proposition 1.1. (a) *$K(\alpha,c)$ and $J(\alpha,c)$ are closed and completely invariant.*
(b) *$K(\alpha,c)$ and $J(\alpha,c)$ are connected if and only if $0 \in K(\alpha,c)$.*
(c) *If $K(\alpha,c)$ is connected, the restriction of f to the complement of $K(\alpha,c)$ is conjugate to the map $z \mapsto z^2$ on the complement of the unit disk.*

Proof. The proof is essentially the same as for quadratic polynomials. Refer to [Douady and Hubbard 1985; Blanchard 1984; Milnor 1990]. □

Proposition 1.2. *Every path component of $K(\alpha,c)$ is simply connected.*

Proof. If γ is a Jordan curve contained in $K(\alpha,c)$, its iterates are bounded. Consider the component

D of $\mathbb{C} \setminus \gamma$ that does not contain infinity. Since $f_{\alpha,c} : \mathbb{C} \to \mathbb{C}$ is an open map, a point in D cannot map to a boundary point of $f^n(D)$ under f^n. Thus $\partial f^n(D) \subset f^n(\partial D) = f^n(\gamma)$, and $f^n(D)$ will then be bounded. Therefore D is contained in $K(\alpha, c)$. $\square$

Define for fixed α the *connectedness locus* $\mathcal{C}_\alpha$ of the family $\{f_{\alpha,c}\}_{c\in\mathbb{C}}$ as

$$\mathcal{C}_\alpha = \{c \mid K(\alpha, c) \text{ is connected}\}.$$

$\mathcal{C}_1$ is known as the Mandelbrot set. An interesting issue is the dependence of $\mathcal{C}_\alpha$ on the parameter. An isolated saddle-node bifurcation that results in an attractor that attracts the critical point could ruin the continuity in the Hausdorff topology. We have not observed such a bifurcation. At this point we formulate the following conjecture:

Conjecture 1.3. *The connectedness locus $\mathcal{C}_\alpha$ varies continuously with α in the Hausdorff topology.*

Remark. Another interesting subset of the parameter space is

$$\mathcal{D}_\alpha = \{c \mid K(\alpha, c) \text{ is not totally disconnected}\}.$$

In the conformal case, $K(\alpha, c)$ is not connected if and only if it is totally disconnected. In Section 2, we show that for large c the set $K(\alpha, c)$ is totally disconnected. In the case where $\alpha < 1$, there are c values for which $K(\alpha, c)$ is not connected and not totally disconnected (see Section 4). It may be that $\mathcal{C}_\alpha = \mathcal{D}_\alpha$ for $\alpha \geq 1$. This is about all we know about $\mathcal{D}_\alpha$. It would be interesting to find a computer algorithm to draw this set.

Besides the Mandelbrot set $\mathcal{C}_1$, the two extreme examples can be fairly well understood.

Proposition 1.4. *The connectedness locus $\mathcal{C}_{1/2}$ is a union of half-lines, containing the origin.*

Proof. Let f_c denote the map $f_{1/2,\,c}$. Then

$$f_{kc}(kz) = kf_c(z)$$

for any $k > 0$. Consider the orbit of the critical point. It is easily seen by induction that $f_{kc}^{n+1}(0) = kf_c^{n+1}(0)$. Therefore the property that the orbit of the critical point be bounded is independent of k. $\square$

Proposition 1.5. *As $\alpha \to \infty$, $\mathcal{C}_\alpha$ converges in the Hausdorff topology to the unit disk.*

Proof. For $|c| > 1$ and α large enough, $f_{\alpha,c}^2(0)$ is close to infinity. Consequently, any Hausdorff limit is contained in the closed unit disk. On the other hand, when $|c| < 1$ and ε is small, the orbit of the critical point is contained in the disk of radius $|c|+\varepsilon$ for α large enough. Therefore any open disk contained in the closed unit disk is contained in $\mathcal{C}_\alpha$ for α large enough. $\square$

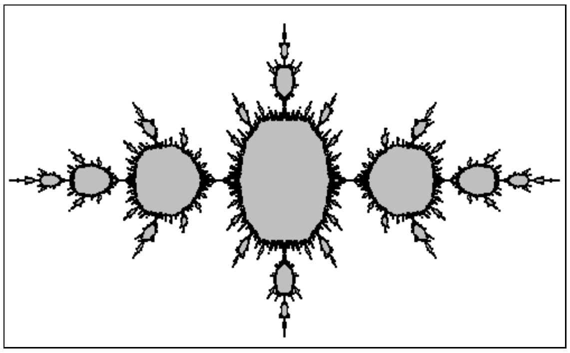

$\alpha = 0.75 \quad c = -0.78 \quad z \in \lfloor -2 - 1.1i,\, 2 + 1.1i \rceil$

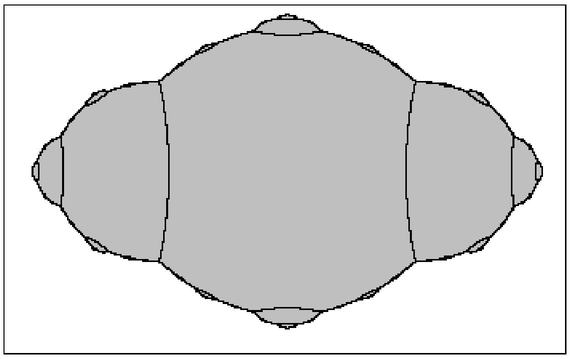

$\alpha = 1.5 \quad c = -0.8 \quad z \in \lfloor -1.4 - i,\, 1.4 + i \rceil$

FIGURE 1. Examples of filled Julia sets $K(\alpha, c)$. Throughout this paper we use the notation $\lfloor a, b \rceil$ to denote the rectangle in $\mathbb{C}$ with a at the lower left corner and b at the upper right.

2. WHEN DISCONNECTED FILLED-IN JULIA SETS ARE CANTOR SETS

In the holomorphic case ($\alpha = 1$), disconnected filled-in Julia sets are totally disconnected. When $\alpha \neq 1$, this need no longer be true. One can find values of the parameter for which there are periodic attractors, while the critical point tends to ∞. These examples have only been found when $\alpha < 1$ (see Section 4). When $|c|$ is large enough for fixed α, this behavior cannot occur:

Theorem 2.1. *If $|c| - |2c|^{1/2\alpha} \geq 1$, then $K(\alpha, c)$ is totally disconnected, $K(\alpha, c) = J(\alpha, c)$ and $f_{\alpha,c}$ is uniformly expanding on $J(\alpha, c)$.*

Proof. The idea of the proof is straightforward. First, we show in the lemma below that there is a disk containing the critical point that iterates to ∞. The next proposition shows that the map on the filled-in Julia set is uniformly expanding; the theorem follows immediately. $\square$

Lemma 2.2. *If $|c| \geq 2^{1/(2\alpha-1)}$, then*

$$\left(|c| - |2c|^{1/2\alpha}\right)^{1/2\alpha} \leq |z| \leq |c|$$

for any $z \in K(\alpha, c)$.

Proof. When $|c| \geq 2^{1/(2\alpha-1)}$, we have $|c|^{2\alpha} \geq 2|c|$. Consider a point z with $|z| > |c|$. Then

$$\begin{aligned} |f_{\alpha,c}(z)| &\geq |z|^{2\alpha} - |c| = (|z/c|^{2\alpha})|c|^{2\alpha} - |c| \\ &> |z/c|(2|c|) - |c| = 2|z| - |c| > |z|. \end{aligned}$$

If the orbit of z remains bounded, the continuity of f implies the existence of a limit point z_∞ of the orbit such that $|f_{\alpha,c}(z_\infty)| = |z_\infty|$, yielding a contradiction. Therefore the orbit of z goes to infinity, and so $z \notin K(\alpha, c)$.

On the other hand, for $|z| < \left(|c| - |2c|^{1/2\alpha}\right)^{1/2\alpha}$, we show that the second iterate of z is outside the disk of radius $|c|$, and hence by the above argument, the orbit of z goes to infinity. We have

$$\begin{aligned} |f^2_{\alpha,c}(z)| &\geq |f_{\alpha,c}(z)|^{2\alpha} - |c| \geq \left||c| - |z|^{2\alpha}\right|^{2\alpha} - |c| \\ &> (|2c|^{1/2\alpha})^{2\alpha} - |c| = |c|. \end{aligned}$$ $\square$

Corollary 2.3. (a) *If $|c| > 2^{1/(2\alpha-1)}$ then $0 \notin K(\alpha, c)$ and thus $c \notin \mathcal{C}_\alpha$.*
(b) *If $c \in \mathcal{C}_\alpha$ and $z \in K(\alpha, c)$, then $|c| \leq 2^{1/(2\alpha-1)}$ and thus $|z| \leq 2^{1/(2\alpha-1)}$.*

Proposition 2.4. *If $|c| - |2c|^{1/2\alpha} \geq 1$, then $f_{\alpha,c}$ expands the Euclidean metric on $K_{\alpha,c}$.*

Proof. Let $f = f_{\alpha,c}$, let z be a point in $K_{\alpha,c}$, let $A = D_z f$, and let v be a nonzero tangent vector in $T_z\mathbb{C}$. We must show that $\langle Av, Av\rangle > \langle v, v\rangle$, or equivalently $\langle A^*Av, v\rangle > \langle v, v\rangle$. Since A^*A has an orthonormal basis of eigenvectors with positive eigenvalues, it suffices to show that the minimum eigenvalue $\lambda_{\min}$ of A^*A is greater than 1.

For general f we have $\lambda_{\min} = (|f_z| - |f_{\bar z}|)^2$, and in our case $\lambda_{\min} = (\alpha + 1 - |\alpha - 1|)^2|z|^{4\alpha-2}$. By Lemma 2.2, we have $|z| \geq (|c| - |2c|^{1/2\alpha})^{1/2\alpha} \geq 1$, since $z \in K_{\alpha,c}$. When $\alpha \geq 1$ we have $\lambda_{\min} = 4|z|^{4\alpha-2} \geq 4$, and when $\frac{1}{2} < \alpha \leq 1$,

$$\lambda_{\min} = 4\alpha^2|z|^{4\alpha-2} \geq 4\alpha^2 > 1.$$ $\square$

3. SMOOTH JULIA SETS

In the holomorphic case there are only two smooth Julia sets. When $c = 0$, the Julia set is the unit circle, and is a hyperbolic set. When the critical value c is real and is one of the preimages of a repelling fixed point, the Julia set is the closed interval between $-|c|$ and $|c|$. This value for c is at the "tip" of the Mandelbrot set, and in this case the dynamics on the Julia set is subhyperbolic (the is, expanding with respect to a metric that is smoothly equivalent to the Euclidean metric except at a finite number of points.)

For fixed values of α, one finds readily the parameter value for which the critical value is a preimage of a repelling fixed point. This fixed point is real and has coordinate $-c$. The fixed point equation is $|c|^{2\alpha} + c = -c$, so $c = -2^{1/(2\alpha-1)}$. We denote the corresponding Julia set by J_α. Numerical observations suggest that when α is between $\frac{1}{2}$ and 2, J_α is indeed an interval, and that when α is greater than 2, J_α is not contained in the real line.

Theorem 3.1. *When α is between 0.5 and 1.7, the Julia set $J_\alpha = J(\alpha, c)$, with $c = -2^{1/(2\alpha-1)}$, is an interval. The dynamics on J_α is subhyperbolic.*

The idea of the proof is straightforward: to find a metric that is contracted by the inverse (branches) of $f_{\alpha,c}$. Consider the metric

$$\rho_\alpha(z)\,|dz| = \frac{|dz|}{|c^2 - z^2|^{(2\alpha-1)/2\alpha}}.$$

The restriction of this metric to the interval $[-c, c]$ was considered by Jiang [1990].

Proposition 3.2. *When $0.5 \le \alpha \le 1.7$, f expands the metric ρ_α on the ball of radius $2^{1/(2\alpha-1)}$.*

Proof. We want to show that $f^*(\rho_\alpha) > \rho_\alpha$. We let $p = (2\alpha-1)/2\alpha$. We have $2c = -|c|^{2\alpha}$ and $f(z) = z^{\alpha+1}\bar{z}^{\alpha-1} + c$. Now

$$\begin{aligned} f^*(\rho_\alpha)(z) &= \frac{|f_z\,dz + f_{\bar z}\,d\bar z|}{\left|c^2 - (|z|^{2\alpha-2}z^2 + c)^2\right|^p} \\ &= \frac{|(\alpha+1)\bar z^{\alpha-2}z^\alpha \bar z\,dz + (\alpha-1)\bar z^{\alpha-2}z^\alpha z\,d\bar z|}{\left|2c|z|^{2\alpha-2}z^2 + z^4|z|^{4\alpha-4}\right|^p} \\ &= \frac{|(\alpha+1)\,dz + (\alpha-1)(z/\bar z)\,d\bar z|}{|z|^{1-2\alpha}\left||z|^{4\alpha-4}z^4 - |c|^{2\alpha}|z|^{2\alpha-2}z^2\right|^p} \\ &= \frac{|(\alpha+1)\,dz + (\alpha-1)(z/\bar z)\,d\bar z|}{\left||z|^{2\alpha-2}z^2 - |c|^{2\alpha}\right|^p}. \end{aligned}$$

We now wish to show that the "expansion" ratio $f^*(\rho_\alpha)/\rho_\alpha$ at a point z in the disk of radius $2^{1/(2\alpha-1)}$ is bounded from below by one. We have

$$\frac{f^*(\rho_\alpha)}{\rho_\alpha} = \left|(\alpha+1) + (\alpha-1)\frac{z}{\bar z}\frac{d\bar z}{dz}\right| \times \left(\frac{|c^2 - z^2|}{\left||c|^{2\alpha} - |z|^{2\alpha-2}z^2\right|}\right)^p.$$

Now let $z = 2^{1/(2\alpha-1)}xe^{i\theta}$. Since z is in the closed disk of radius $2^{1/(2\alpha-1)} = |c|$, we have $0 \le x \le 1$. Denote by $e^{i\varphi}$ the quantity $d\bar z/dz$. We can express the expansion ratio as the product of two terms. The first is

$$|(\alpha+1) + (\alpha-1)e^{i(2\theta+\varphi)}|,$$

which is bounded below by 2α when $\alpha \le 1$ and by 2 when $\alpha \ge 1$. The second term is

$$\left(\frac{|2^{2/(2\alpha-1)}(1 - e^{2i\theta}x^2)|}{|2^{2\alpha/(2\alpha-1)}(1 - e^{2i\theta}x^{2\alpha})|}\right)^p = 2^{(1-\alpha)/\alpha}\left(\frac{|1 - e^{2i\theta}x^2|}{|1 - e^{2i\theta}x^{2\alpha}|}\right)^p.$$

The term in parentheses on the right exceeds α^{-1} when $\alpha > 1$, and exceeds $\frac{1}{2}$ when $\alpha \le 1$. Hence, for $\alpha > 1$, the expansion factor is greater than $2^{1/\alpha}\alpha^{-(2\alpha-1)/2\alpha}$, which is a decreasing function of α and is bigger than 1 for all $\alpha \in [1, 1.7]$. For $\alpha < 1$, the expansion factor is greater than $\alpha\, 2^{(3-2\alpha)/2\alpha}$, which is also a decreasing function of α, and is greater than 1 when $\alpha = 1$. We conclude that when $.5 \le \alpha \le 1.7$, the ratio $f^*(\rho_\alpha)/\rho_\alpha$ is uniformly greater than one for all points z within the disk of radius $2^{1/(2\alpha-1)}$. □

Proof of Theorem 3.1. By Corollary 2.3, the filled-in Julia set is contained in the closed disk D of radius $2^{1/(2\alpha-1)}$. From the proof of Lemma 2.2, it follows that the inverses of f map this disk into itself. Let S_0 and S_1 be the two components of the inverse image of the disk:

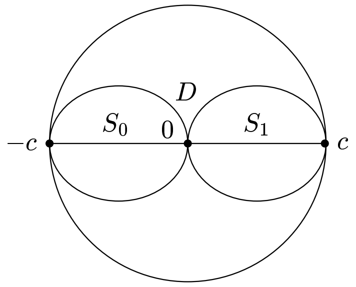

The two inverse branches $\psi_i\colon D \to S_i$ are homeomorphisms; by the previous proposition, they are uniformly contracting. Thus, the diameter of the sets $\psi_{\varepsilon_1} \circ \psi_{\varepsilon_2} \circ \cdots \circ \psi_{\varepsilon_n}(D)$ go to 0 geometrically. Hence, there is exactly one point x_ε with the n-th iterate of x_ε in S_{ε_n}, where $\varepsilon = (\varepsilon_1, \varepsilon_2, \ldots)$ (preimages of the critical value have two such representations ε). For each ε there is a point on the real segment with the itinerary ε, and so there are no other points in the filled-in Julia set. □

Conjecture 3.3. *For all α in $(\frac{1}{2}, 2)$, the Julia set J_α is the interval $(-2^{1/(2\alpha-1)}, 2^{1/(2\alpha-1)})$, and the dynamics on J_α is subhyperbolic.*

Structural Stability

We now investigate structurally stable properties for α fixed and c near zero. Consider $f_c = f_{\alpha,c}$. Take c to be zero. The unit circle S^1 is smooth, f_0-invariant and repelling. In fact $T_{S^1}\mathbb{C}$ splits as a direct sum $TS^1 \oplus N$ of invariant bundles, where N corresponds to the radial direction. We have $|Df_0(v)| = 2\,|v|$ when $v \in TS^1$ and

$$|Df_0(v)| = 2\alpha\,|v|$$

when $v \in N$. If we set $m = \ln(2\alpha)/\ln 2$, the dynamics near S^1 is m-normally hyperbolic in the sense of Hirsch–Pugh–Shub [Hirsch et al. 1977].

On $\mathbb{C} \setminus \{0\}$, we have the foliation by concentric circles and the foliation by radial lines. These foliations are invariant (that is, every component of f_0^{-1} of a leaf is contained in a leaf), smooth, and intersect transversely. We consider the stability properties of these foliations.

Definition. Let A be an annulus. A foliation on A is *circular* if each of the boundary components of A are leaves and if every leaf is homeomorphic to a circle. A foliation on A is *transverse* if every leaf is homeomorphic to a closed interval and intersects each of the boundary components of A in a single point. We say that a circular or transverse foliation on A is C^k when each leaf is C^k-diffeomorphic to a round circle or interval, respectively, and nearby leaves are C^k-close.

Let A and B be domains in the plane. Let $f : B \to A$ be a smooth nonsingular map. Then any foliation on A lifts to a foliation on B. We say that a (C^k) foliation on A is *compatible with the dynamics* if it and its lift to B form a (C^k) foliation of $A \cup B$.

Consider a concentric annulus A containing S^1. Then $f_0^{-1}(A)$ is strictly contained in A. Choose a circular foliation on $A_0 = A \setminus f_0^{-1}(A)$ that is C^k-close to the foliation by round circles (in particular, transverse to the radial foliation). We can obtain a foliation on $A \setminus S^1$ by repeatedly pulling back by f_0^{-1}; adding S^1 gives an f_0-invariant foliation A whose leaves are Jordan curves.

One easily shows that every leaf of this foliation is a graph of a radial function $(r(\theta), \theta)$; these graphs are uniformly C^k for all $k \le \ln(2\alpha)/\ln 2$. The leaves on

$$A_n = A \setminus f_0^{-n-1}(A)$$

converge to the round circle in the C^k topology (Figures 2 and 3).

Now consider a foliation of $A \setminus f_0^{-1}(A)$ by smooth arcs running from one boundary component to another in each component annulus, transverse to the foliation by round circles and compatible with the dynamics. Pull back by the dynamics to obtain a foliation of $A \setminus S^1$ by smooth curves that is transverse to the circular foliation. Since f_0^{-1} is a contraction, each of these curves limits on S^1, and at least two curves land at each point of S^1, one from the inside and one from the outside. Moreover, each of these curves is an angular graph $(r, \theta(r))$ and is uniformly of class C^k for all $k \le (\ln 2)/\ln(2\alpha)$. If $\alpha < 1$, the resulting foliation extends to all of A and all leaves are uniformly C^k for all $k < \ln(2\alpha)/\ln 2$. However, if $\alpha > 1$ and the initial foliation is not exactly radial, the curves cannot meet smoothly at S^1. See Figure 4.

Theorem 3.4. *Fix $\alpha \neq 1$ and a concentric annulus A containing the unit circle in its interior, and let $m = \ln(2\alpha)/\ln 2$.*

(a) *If $\alpha > 1$, then for all $k < m$ there exists δ_k so that, when $|c| < \delta_k$, any initial circular C^k foliation on $A \setminus f_c^{-1}(A)$ that is close to the round foliation will pull back and extend to an f_c-invariant C^k foliation on A.*

(b) *If $\alpha < 1$, then for all $k < m^{-1}$ there exists δ_k so that, when $|c| < \delta_k$, any C^k transverse foliation on $A \setminus f_c^{-1}(A)$ that is close to the radial foliation and dynamically compatible will pull back and extend to an f_c-invariant C^k foliation on A.*

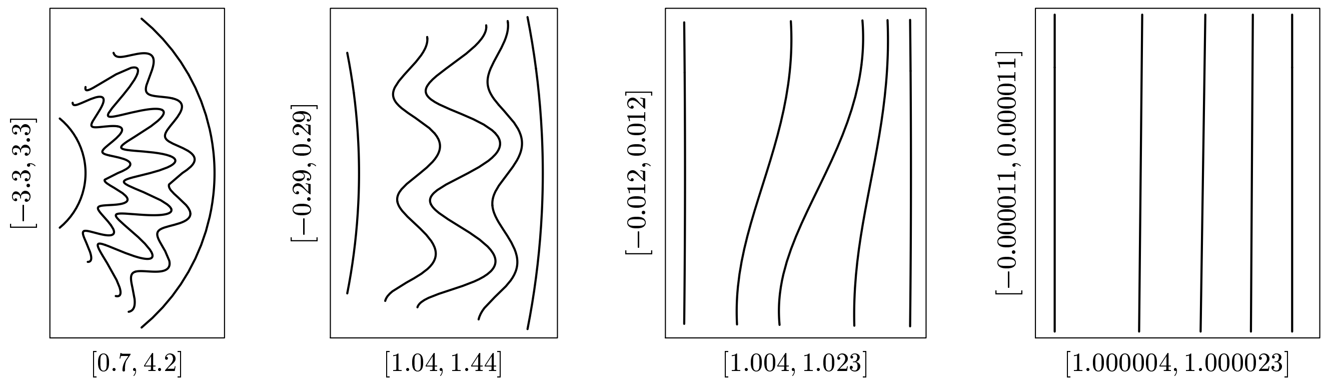

FIGURE 2. Part of several leaves of a circular foliation on the outer component of A_0, and the pullbacks to A_1, A_3, and A_8 when $\alpha = 2$. These leaves converge to the round circle in the C^2 topology.

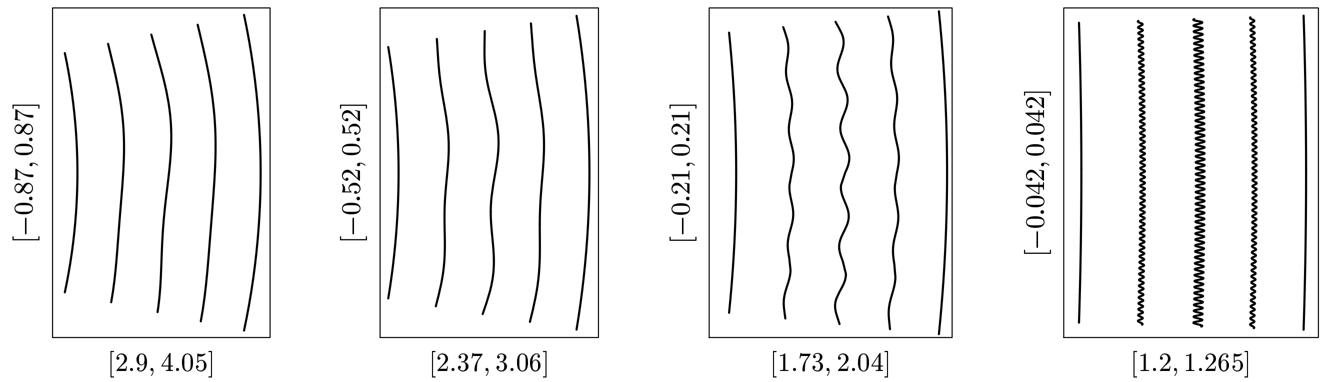

FIGURE 3. Leaves of a circular foliation on the outer component of A_0, and pullbacks to A_1, A_3, and A_8 when $\alpha = \frac{5}{8}$. The convergence to the circle is only C^0.

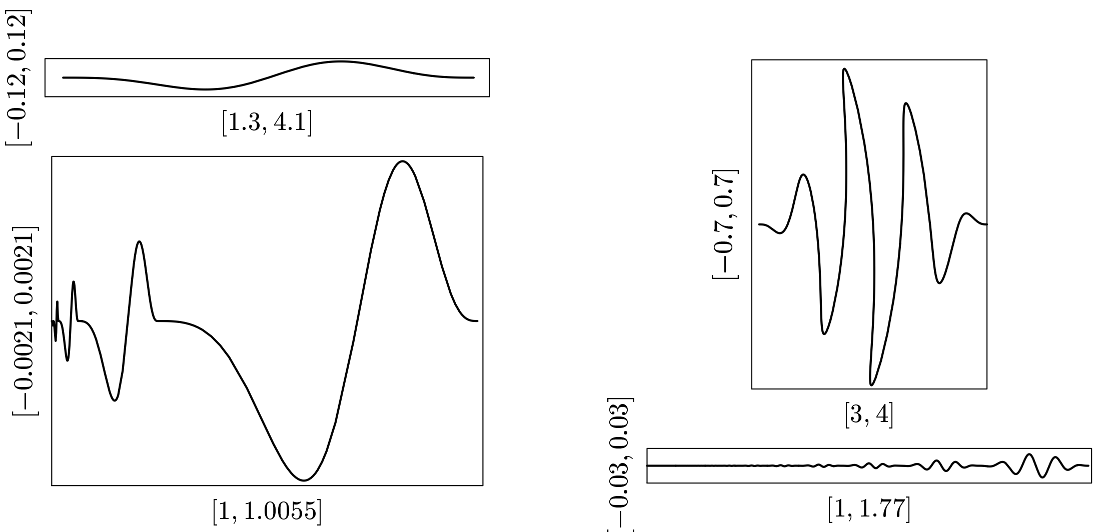

FIGURE 4. The top two graphs show a leaf of a transverse foliation on the outer component of A_0, for $\alpha = 2$ (left) and $\alpha = \frac{5}{8}$ (right). The bottom two show the corresponding leaves in the outer component of $\bigcup_{n=3}^{\infty} A_n$. For $\alpha = 2$, although the initial leaf is close to being radial, it becomes less so under iteration; in particular, notice the lack of smoothness near the limit at $(1, 0)$. For $\alpha = \frac{5}{8}$, on the contrary, we chose an initial foliation that is far from radial, but the result under iteration has a C^3 limit that is exactly radial.

Corollary 3.5. (a) *If $\alpha > 1$ and $|c| < \delta_k$, the Julia set $J(\alpha, c)$ is a C^k curve.*

(b) *If $\alpha < 1$ and $|c| < \delta_k$, the Julia set $J(\alpha, c)$ intersects every leaf of the corresponding radial foliation in a single point.*

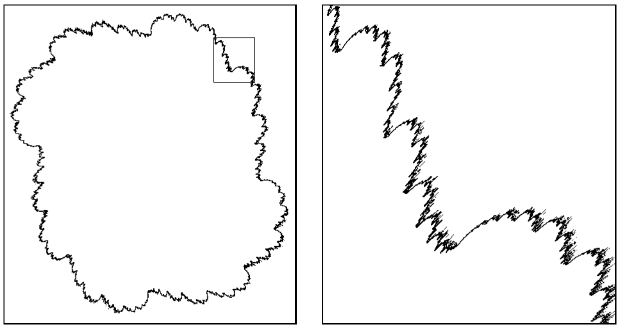

$\lfloor -1.1 - 1.2i,\ 1.1 + 1.2i \rceil$ $\lfloor .48 + .62i,\ .79 + .958i \rceil$

FIGURE 5. The Julia set $J(0.75,\ 0.1 + 0.1i)$ and a blowup of it. This illustrates Corollary 3.5: although the Julia set is not at all smooth, it looks like the graph of a polar function $r = f(\theta)$.

Proof of Theorem 3.4. Most of the technical details can be found in [Hirsch et al. 1977] (diffeomorphisms). Since the maps we discuss here have degree two, the initial setup is a little bit different. Consider the following cone fields on $\mathbb{C} \setminus \{0\}$:

$$C^+(r, \theta) = \left\{ R\frac{\partial}{\partial r} + \Theta\frac{\partial}{\partial \theta} \;\middle|\; |R| \le |\Theta| \right\},$$

$$C^-(r, \theta) = \left\{ R\frac{\partial}{\partial r} + \Theta\frac{\partial}{\partial \theta} \;\middle|\; |R| \ge |\Theta| \right\}.$$

When $\alpha > 1$, f_0^{-1} maps C^+ strictly into itself. Consider the annulus A. For $|c|$ small enough, f_c^{-1} maps the cone field C^+ on A strictly into itself. Choose an initial circular foliation on $A_0 = A \setminus f_c^{-1}(A)$ where the tangent vectors at each point are in the cone C^+, and extend this to a foliation $\mathcal{F}_0$ on all of A which has the same property. Define a new foliations $\mathcal{F}_1$ as follows: pull back $\mathcal{F}_0$ on A_0 by f_c^{-1} to obtain a foliation on $A_1 = A \setminus f_c^{-2}(A)$. Extend this to all of A as before to obtain $\mathcal{F}_1$. Iterate this procedure to obtain a sequence of circular foliations $\mathcal{F}_n$ on A.

Now choose $k < m$, and assume that the leaves of $\mathcal{F}$ are C^k. The techniques in [Hirsch et al. 1977] show that when $|c|$ is small enough, the sequence $\mathcal{F}_n$ is C^k-compact and therefore has a limit point $\mathcal{F}_\infty$ that only depends on the choice in $A \setminus f_c^{-1}(A)$. Since the foliations $\mathcal{F}_n$ agree on larger and larger domains, $\mathcal{F}_\infty$ is the only limit point. In particular, the Julia set $J(\alpha, c)$ is C^k.

When $\alpha < 1$, the situation is reversed: the cone field C^- is mapped into itself by f_0^{-1}. When $|c|$ is sufficiently small, f_c^{-1} restricted to A maps C^- into itself. Now consider a transverse foliation on $A - f_c^{-1}(A)$ that is dynamically compatible and whose tangent-line field is in the cone field C^-. Extend this foliation to all of A so that the tangent-line field is in the cone field everywhere. Repeat the pull-back construction. When $k < m^{-1}$ this gives a C^k-compact sequence of transverse foliations on A, for $|c|$ sufficiently small. Again, there is a single limit point which only depends on the initial choice in $A \setminus f_c^{-1}(A)$.

We finally argue that the Julia set intersects every leaf in exactly one point. The Julia set $J(\alpha, c)$ certainly intersects every leaf in at least one point. If it intersects in say two points, we can iterate forward and conclude that there are points of the Julia set in $A \setminus f_c^{-1}(A)$. This is a contradiction. $\square$

Since the construction of the foliations in Theorem 3.4 involves choices, one may ask if it is possible to make canonical choices. This is indeed the case on the unbounded component of the complement of the Julia set. Construct an invariant foliation near infinity and pull back by the dynamics. For $\alpha > 1$ one can then make a canonical choice of C^k circular foliation on the closure of the unbounded component, and for $\alpha < 1$ one can make a canonical choice of C^k transverse foliation. It is interesting that this construction is also possible when $\alpha = 1$, the conformal case. Though Theorem 3.4 no longer holds in this case, one still obtains foliations, but by quasicircles and quasiarcs (radial lines and equipotential lines), rather than by C^k curves [Douady and Hubbard 1985].

Remark. Jiang [1990] has shown that for all $c \neq 0$ with $|c|$ sufficiently small, there is a $\tau_c > 0$ such that for α with $1 - \tau_c \leq \alpha \leq 1 + \tau_c$, the Julia set $J(\alpha, c)$ has Hausdorff dimension greater than 1 (Figure 6).

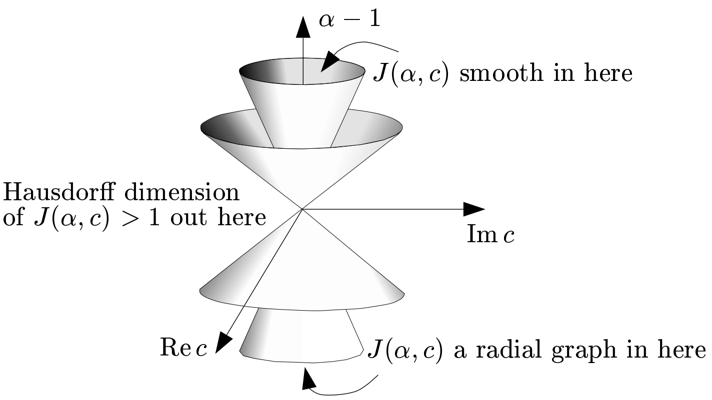

FIGURE 6. Schematic classification of the smoothness of the Julia sets near the map $z \mapsto z^2$ in α-c parameter space.

4. FIXED POINTS

In the holomorphic case ($\alpha = 1$) there is one component of the interior of the connectedness locus that one can understand in all detail, namely, the period-one component. For each parameter value there, the corresponding map has a single attracting fixed point, which moreover attracts the critical point. This component is a disk and its boundary is a cardioid. For every parameter value in this boundary the corresponding map has a neutral fixed point. When the eigenvalue of this fixed point is a root of unity $e^{2\pi i p/q}$ (with p and q relatively prime), the corresponding parameter value occurs at the intersection of the closures of two connected components of the interior of the Mandelbrot set, namely the period-one component and a component where there is a periodic attractor of period q.

In part, the key to this picture is the study of the Leau bifurcation [Milnor 1990]. Here one considers the holomorphic one-parameter family of holomorphic germs defined near the origin:

$$P_\lambda(z) = \lambda z + z^2 h(z), \quad P_\lambda(0) = 0,$$

when λ is in the neighborhood of a root of unity. This study of the period-one component applies to other hyperbolic components as well. If one considers a component for which one has a periodic attractor of period q, at each point of the boundary of this component one has a neutral periodic cycle, and taking the q-th iterate reduces the study of the bifurcation to that of the Leau bifurcation. In particular, the boundary of such a component is an algebraic curve.

When $\alpha \neq 1$ our understanding is already incomplete for the period-one component, which we define as the set of parameters c in the connectedness locus for which $f_{\alpha,c}$ has an attracting fixed point. Moreover, the analysis we carry out in the period-one component does not automatically extend to the components corresponding to periodic attractors of higher period. We show below that when $\alpha \neq 1$ and an attractor is present, the critical point is not necessarily attracted to it.

Fix α. We first analyze the fixed-point picture. For every z_0, there is a c such that z_0 is a fixed point of $f_{\alpha,c}$, namely,

$$c = z_0 - z_0^{\alpha+1} \bar{z}_0^{\alpha-1}.$$

If z_0 is a fixed point of $f_{\alpha,c}$, the derivative $D(z_0)$ of $f_{\alpha,c}$ at z_0 is

$$(\alpha+1) z_0^{\alpha} \bar{z}_0^{\alpha-1} dz + (\alpha-1) z_0^{\alpha+1} \bar{z}_0^{\alpha-2} d\bar{z}.$$

The point z_0 is an attracting fixed point if the eigenvalues of $D(z_0)$ are both in the unit disk. In the closure of the set of such attracting fixed points, there are three important curves:

- δ where $\det D(z_0) = 1$;
- γ_+ where $D(z_0)$ has an eigenvalue $+1$;
- γ_- where $D(z_0)$ has an eigenvalue -1.

Figure 7 shows these curves for several values of α.

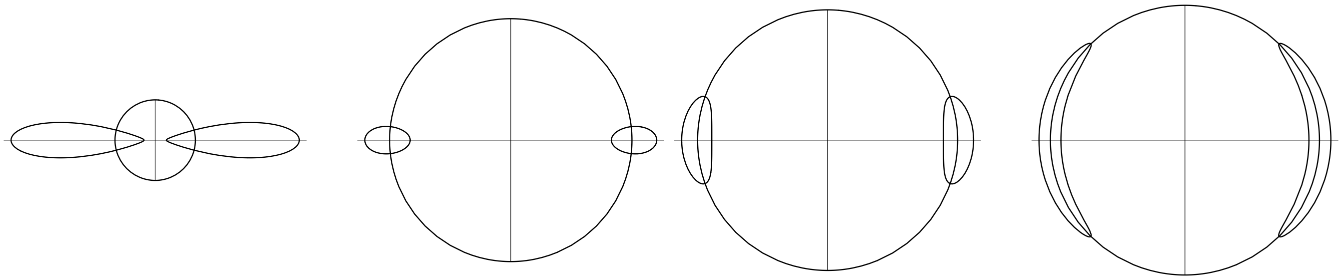

$\alpha = 0.6 \quad r = 0.11206$ $\qquad \alpha = 0.8 \quad r = 0.37935$ $\qquad \alpha = 2.0 \quad r = 0.70711$ $\qquad \alpha = 6.0 \quad r = 0.86549$

FIGURE 7. The curves γ_-, δ (a circle of radius r) and γ_+, for various values of α.

A point $z_0 = r_0 e^{i\theta_0}$ is on δ if and only if

$$\det D(z_0) = 4\alpha r_0^{4\alpha-2} = 1,$$

and therefore δ is a circle of radius $(4\alpha)^{1/(2-4\alpha)}$.

A point z_0 is on γ_+ if and only if

$$1 - \operatorname{tr} D(z_0) + \det D(z_0) = 0,$$

or, equivalently,

$$1 - 2(\alpha+1) r_0^{2\alpha-1} \cos\theta_0 + 4\alpha r_0^{4\alpha-2} = 0.$$

We claim that γ_+ is a smooth simple closed curve. There are at most two values of $r_0^{2\alpha-1}$ satisfying the preceding equation. Because we want to consider only the solutions for r_0 positive, we must have $\cos\theta_0 \geq 0$. Moreover, the discriminant of the equation is nonnegative when $\cos^2\theta_0 > 4\alpha/(\alpha+1)^2$, that is, in an angular sector about the real axis (when $\alpha = 1$, this sector reduces to a single point). The discriminant vanishes at the ends of that angular sector. Consequently, γ_+ is a topological circle. One can check that the curve is C^1.

The curves γ_+ and δ intersect in two points (only one when $\alpha = 1$). Notice that $\gamma_- = -\gamma_+$, because z_0 is on γ_- if and only if $1 + \operatorname{tr} D(z_0) + \det D(z_0) = 0$.

Define $P_1(\alpha)$ as the locus of c such that $f_{\alpha,c}$ has an attracting fixed point. The previous analysis immediately provides us with insight about $P_1(\alpha)$. Consider the map $p : \mathbb{C} \to \mathbb{C}$ that assigns to each z the parameter value that makes z a fixed point: $f_{p(z)}(z) = z$. Explicitly, we have

$$p(z) = z - z^{\alpha+1}\bar{z}^{\alpha-1}.$$

When z is real, $p(z)$ is real and p commutes with conjugation. One checks that p is injective on $\gamma_\pm$, injective on δ when $\alpha \geq 1$, and has a single point of multiplicity two on δ when $\alpha < 1$.

We will now discuss the dynamics of the fixed points $z_0 \in p^{-1}(c)$ for c in $\mathbb{C}$. We present the outcome first, followed by a partial analysis. The bifurcations occur along the curves $p(\gamma_\pm)$ and $p(\delta)$ (Figure 8). One can show that, for $\alpha \neq 1$, $p(\delta)$ is a limaçon, $p(\gamma_-)$ is diffeomorphic to a circle, and $p(\gamma_+)$ is a simple closed curve with three cusps. Three qualitatively different partitionings of the c-plane are possible, depending on whether α is less than, equal to, or greater than 1 (Figures 9–11).

The case $\frac{1}{2} < \alpha < 1$

Here the limaçon $p(\delta)$ has an inner loop. We describe the fixed points occurring in each region of Figure 9 (see the caption of that figure for the meaning of $+$, $\bullet$ and $\circ$). We draw attention to the possibility of attracting fixed points that fail to attract the critical point (regions $\overset{\bullet}{\bullet}$ and $\circ{+}$).

$\overset{\circ}{\circ}$ Outside the limaçon $p(\delta)$ and outside $p(\gamma_-)$, there are always two repelling fixed points.

$\circ{+}\overset{\bullet}{\bullet}$ Inside $p(\gamma_+)$ there are four components cut out by the limaçon. Region $\circ{+}\overset{\bullet}{\bullet}$ is given by the two pieces that intersect the real line. There are two attracting points, one repelling point, and one saddle. Part of the curve $p(\delta)$ crosses this region, but crossing this curve only changes the product of the eigenvalues of the saddle from less than one to greater than one; no bifurcation occurs.

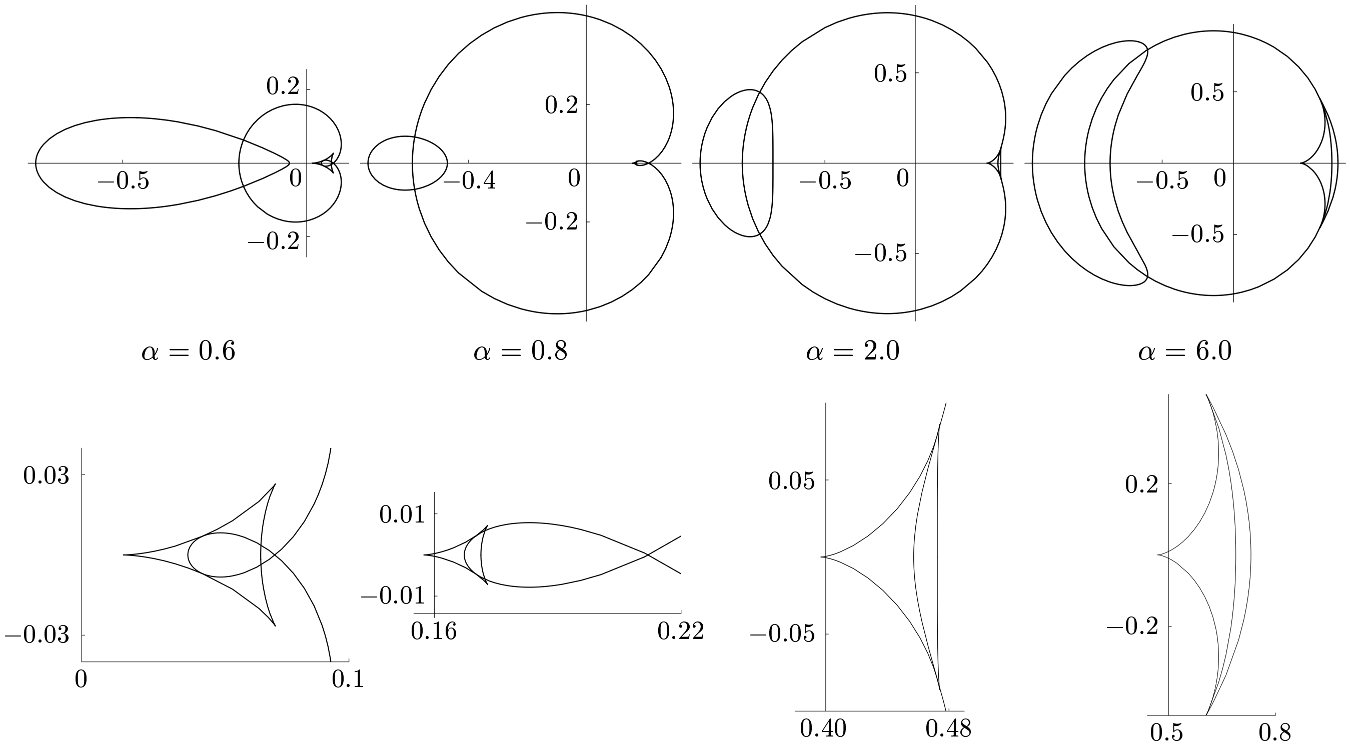

FIGURE 8. The curves $p(\gamma_-)$ (leftmost in each top diagram), $p(\delta)$ and $p(\gamma_+)$ (three-cusped, and magnified in bottom diagram), for various values of α.

8+• This region consists of the two components inside $p(\gamma_+)$ that do not intersect the real line; here there is one attracting fixed point, a saddle, and two repelling fixed points. Crossing the curve $p(\delta)$ into region ∘+: causes one of the repelling points to undergo a Hopf bifurcation (see below) and become attracting. As one crosses the curve $p(\gamma_+)$ into the ∘• region, a saddle and repelling fixed point collide and cancel.

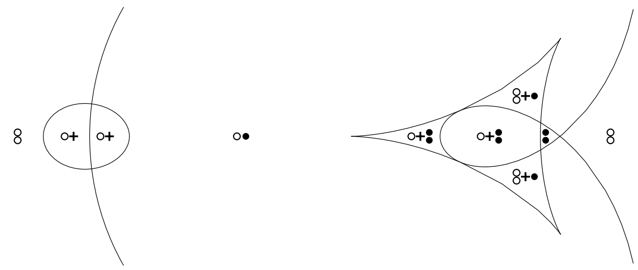

FIGURE 9. Fixed-point behavior for $\frac{1}{2} < \alpha < 1$. For each region in the c-plane delimited by the curves $p(\delta)$, $p(\gamma_+)$ and $p(\gamma_-)$ we indicate the number and types of fixed points that exist there: • represents an attracting fixed point, ∘ a repelling fixed point, and + a saddle. The top and bottom of the limaçon $p(\delta)$ have been clipped, and the region on the right has been magnified.

: Outside $p(\gamma_+)$ but inside the inner loop of the limaçon we have two attracting fixed points. When one crosses $p(\delta)$ into region ∘•, one of the attracting points becomes repelling, generally with a Hopf bifurcation. Entering this region from ∘+: causes the repelling point and the saddle to cancel. Since there are two attracting fixed points, there must be at least one that doesn't attract the critical point. In fact, when c is real the critical point iterates to infinity.

∘+ Inside $p(\gamma_-)$ there is always one repelling fixed point and one saddle. As above, the part of the $p(\delta)$ inside this region doesn't cause a bifurcation. For c real near $p(\gamma_-)$, there is a period-two attractor that fails to attract the critical point; it is attracted to the saddle instead. As one leaves this region into region 8, the saddle splits into a repelling fixed point and a period-two saddle.

○● In this region, which is inside the main loop of the limaçon, we have one attractive and one repelling fixed point. When one enters this region from region ○+:, one of the attracting points and the saddle collide and cancel. When one enters from region ○+, the saddle merges with a period-two attractor and an attracting fixed point is created. When one crosses into 8, the attracting fixed point becomes repelling and typically a Hopf bifurcation occurs. We will discuss the direction of the Hopf bifurcation at the end of this section.

The case $\alpha = 1$

In the conformal case, $p(\delta)$ is a cardioid and $p(\gamma_+)$ and $p(\gamma_-)$ are points on the real axis (Figure 10).

○● Inside the cardioid there is one attracting and one repelling fixed point. The system being conformal, the critical point is in the attractor's basin.

8 Outside the cardioid there are two repelling fixed points. In this case no Hopf bifurcation can occur; when going through a point on the cardioid for which the derivative at the fixed point is of the form $e^{2\pi i p/q}$, a Leau–Fatou flower bifurcation occurs [Milnor 1990].

The case $\alpha > 1$

Here the limaçon is convex or has a dimple. We conjecture, based on numerical evidence, that the critical point is attracted to the attractive point when it exists.

8 Outside the limaçon and outside $p(\gamma_\pm)$ there are two repelling fixed points.

8+• The limaçon cuts $p(\gamma_+)$ into four pieces. The two pieces intersecting the real line form region 8+•, which has two repelling fixed points, one attracting fixed point, and one saddle point. As for $\alpha < 1$, crossing $p(\delta)$ inside this region doesn't cause a bifurcation. When crossing $p(\gamma_+)$ into region 8, the attracting fixed point and the saddle collide; crossing into region ○● causes one of the repelling fixed points and the saddle to collide.

○+: This tiny region consists of the two components inside both $p(\gamma_+)$ and $p(\delta)$ that do not intersect the real line. Here there are two attracting fixed points, one repelling, and one saddle point. When moving from here to region ○● an attracting fixed point and a saddle cancel. When moving from here to region 8+•, one of the attracting fixed points loses stability and becomes repelling, generally via a Hopf bifurcation.

○+ Inside $p(\gamma_-)$ we have one saddle point and one repeller. As before, crossing $p(\delta)$ inside this region causes no bifurcation. When crossing into 8, the saddle splits into a period two saddle and a repelling fixed point.

○● Inside the limaçon and outside $p(\gamma_\pm)$ there is one attracting and one repelling fixed point. When one crosses $p(\gamma_+)$ from region 8+•, one of the repelling fixed points and the saddle collide. When one crosses from region ○+ to here an attracting period-two orbit merges with the saddle to form an attracting fixed point.

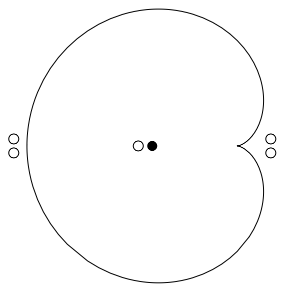

FIGURE 10. Fixed-point behavior when the map is conformal ($\alpha = 1$). The labeling conventions are as in Figure 9.

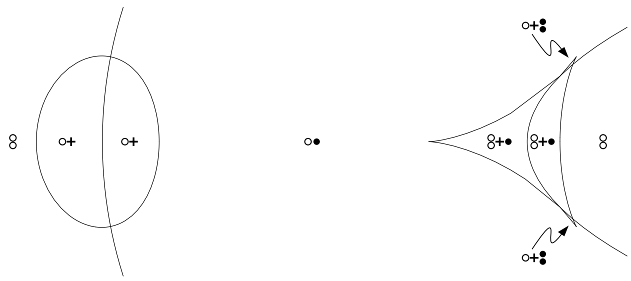

FIGURE 11. Fixed-point behavior for $\alpha > 1$. The conventions (labeling, clipping, different scales) are as in Figure 9.

Justification

We now give the analysis that leads to the bifurcation pictures above. We first consider the case where c is real.

Proposition 4.1. *If c is real, $f_{\alpha,c}$ has at most four fixed points.*

Proof. The point $re^{i\theta}$ is a fixed point if and only if

$$re^{i\theta} - r^{2\alpha}e^{2i\theta} = c.$$

Looking at the imaginary part, we see that

$$r\sin\theta - 2r^{2\alpha}\sin\theta\cos\theta = 0,$$

so either $\sin\theta = 0$ or $r = 2r^{2\alpha}\cos\theta$. In the first case there are two real solutions if c is less than c_0, where $f_{\alpha,c_0}(x)$ is tangent to $y = x$. In the second case we obtain $r^{2\alpha} = c$ after substituting into the real part of the original equation, and thus we get at most one value for r. Substituting this value for r into the original equation gives a quadratic equation in $e^{i\theta}$ that has a solution for every c greater than a certain $c_1 < c_0$. □

We can explicitly calculate the types of the fixed points on the real line: the only way the types or total number of such fixed points can change is when we cross one of the curves $p(\delta)$ or $p(\gamma_\pm)$. Assuming these curves intersect as discussed earlier, the types occurring in each region can be calculated by considering all possible bifurcations. We know that $p(\delta)$ is a limaçon. The difficult part of the analysis is then to figure out how the curves $p(\gamma_\pm)$ cross the limaçon. First we show that $p(\gamma_-)$ intersects the limaçon as shown in the figures, by showing that p is injective on the left half plane.

Proposition 4.2. *The function p is injective on the left half plane.*

Proof. Observe that $p : \mathbb{C} \to \mathbb{C}$ is proper and surjective. Consequently, p maps closed sets to closed sets. Let $\mathfrak{L} = \{z \mid \operatorname{Re} z \le 0\}$ denote the closed left half-plane. Note that p maps the negative real axis onto itself and the imaginary axis onto a parabola-shaped curve that intersects only at the origin:

$$p(iy) = |y|^{2\alpha} + iy.$$

Since p has no singularities on $\mathfrak{L}$, it is an open, orientation-preserving map on $\mathfrak{L}$. In particular, $p(\mathring{\mathfrak{L}})$ is open. Since $p(\mathfrak{L})$ is closed, we conclude that $p(\mathring{\mathfrak{L}})$ is contained in the component of the complement of the image of the imaginary axis that contains the negative real axis. Thus $p(\mathfrak{L})$ is the closure of this component, since $p(\mathfrak{L})$ is closed. The map p is proper on $\mathfrak{L}$, and maps $\mathfrak{L}$ onto this component, so the degree of p is well defined. Since $p^{-1}(0) = \{0\}$, this degree is one. We conclude that p maps the left half plane diffeomorphically onto the component described before. □

Next we must show that $p(\gamma_+)$ intersects the limaçon $p(\delta)$ as indicated in the pictures. This follows from the examination of three types of point:

The images of the two intersections of γ_+ and δ: here Dp has 0 as a double eigenvalue, and the rank is one, as can be seen by explicit computation. This explains the two tangencies between $p(\delta)$ and $p(\gamma_+)$.

The points where the tangent to γ_+ is in the kernel of Dp: one checks that there are exactly three such points, one real (c_1 in the proof of Proposition 4.1) and the other two complex conjugates. This explains the three cusps.

The points where the tangent to γ_+ is horizontal or vertical: one calculates that there is only one point, c_1, where the tangent is horizontal. When $\alpha < 2$ there is only one point (c_0 in the proof of Proposition 4.1) where the tangent is vertical.

It is not hard to show that $p(\gamma_+)$ and $p(\gamma_-)$ do not intersect.

Hopf Bifurcation

Consider a small disc D with center $c_0 \in \delta$ with Df_{c_0} having complex conjugate eigenvalues of absolute value 1 at one fixed point. We wish to discuss the bifurcation picture in this disc. For c in this disc, we can smoothly parametrize the corresponding fixed point $z(c)$ in such a way that $z(c_0) = z_0$. When D is small enough this map $z : D \to \mathbb{C}$ is a diffeomorphism. In particular, $z(D)$ intersects δ, and $D \setminus \delta$ consists of two regions, one where the fixed point is attracting and one where it is repelling. On the boundary of these regions the fixed point is neutrally stable. One should in general expect a Hopf bifurcation, that is, as c passes through the curve δ, the fixed point z_0 will change stability and an invariant circle will be created or destroyed [Marsden and McCracken 1976; Devaney 1989]. This behavior is more precisely described in terms of normal forms, as follows:

Assume that we have chosen z_0 so that its eigenvalues are nonresonant: not first, second, third, or fourth roots of unity. Then one can find new coordinates with respect to which $f_{\alpha,c}$ has the form

$$F_c(z) = \lambda_c z(1 + v_c|z|^2) + O(z^5)$$

around z_0, and whose relationship to the old coordinates depends smoothly on the parameter $c \in D$ [Marsden and McCracken 1976]. (The eigenvalue λ_c and the coefficient v_c depend also on α.) The map $c \mapsto \lambda_c$ is a diffeomorphism on D and intersects the unit circle. The bifurcation theory for c near c_0 depends on $\operatorname{Re} v_{c_0}$, provided $\operatorname{Re} v_{c_0} \neq 0$.

Claim 4.3. *Assume that the eigenvalue λ_{c_0} is nonresonant. Then $\operatorname{Re} v_{c_0} > 0$ for $\frac{1}{2} < \alpha < 1$ and $\operatorname{Re} v_{c_0} < 0$ for $\alpha > 1$. In the conformal case ($\alpha = 1$), v_{c_0} vanishes.*

Justification. When $\alpha = 1$ this is obvious. For other values of α we have found no easy proof. The only more or less straightforward case is an infinitesimal computation near the holomorphic case $\alpha = 1$. Conceivably, a computer-assisted proof of this could be done using interval arithmetic. However, we feel this claim does not merit the effort of a difficult and tedious proof, and have used Mathematica [Wolfram 1988] to perform the coordinate changes and compute v_{c_0} on a large grid of parameter values (see Figure 12). For $\alpha < 1$ we obtained (numerically) $\operatorname{Re} v_{c_0} > 41.487$, and for $\alpha > 1$ we obtained $\operatorname{Re} v_{c_0} < -8.594$. □

By Claim 4.3, the sign of $\operatorname{Re} v_{c_0}$ depends only on α, so we know in which direction the Hopf bifurcation

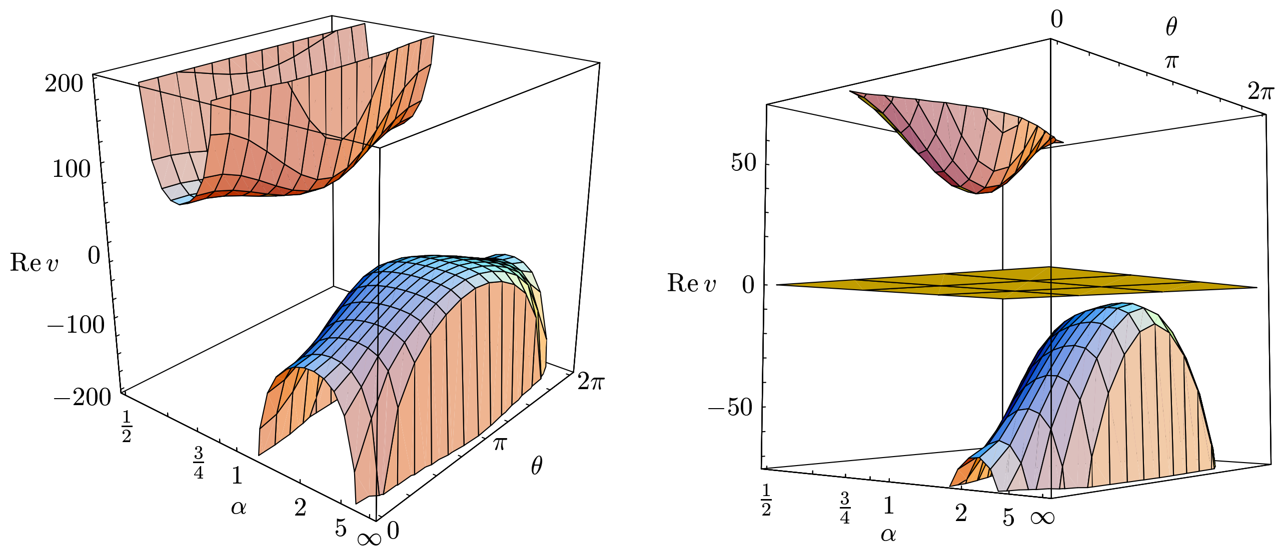

FIGURE 12. Graphs of $\operatorname{Re} v_{c_0}$ as a function of α and $\theta = \arg \lambda_{c_0}$. We have modified the α scale so that the intervals $(\frac{1}{2}, 1)$ and $(1, \infty)$ have the same length. On the right is a closeup near the α-θ plane, which we have shaded to emphasize the plausibility of the claim.

occurs. Assuming that the disc D is small enough, we have the following dichotomy:

When $\alpha < 1$ and $|\lambda_c| < 1$, there exists an invariant circle near $z(c)$ that is repelling in the normal direction. For λ_c outside the closed unit disc, there is no invariant circle near the point $z(c)$.

When $\alpha > 1$, we have the opposite situation: for $|\lambda_c| < 1$, there is no invariant circle close to $z(c)$, and for λ_c outside the closed unit disc, there exists an invariant circle that is attracting in the normal direction. We conjecture that the critical point is still attracted to this circle.

5. Remarks on the Topology of the Connectedness Locus

In the holomorphic case ($\alpha = 1$), the connectedness locus is called the Mandelbrot set, and is connected [Douady and Hubbard 1985]; its complement in the Riemann sphere is conformally equivalent to the open disk. Every connected component of its interior is a topological disk, and is either a *hyperbolic component* or a *queer component*. For any map lying in a hyperbolic component, there is a periodic attractor that necessarily attracts the critical point. Each hyperbolic component has a *center*—the parameter value for which the critical orbit is periodic. Within any component, hyperbolic or not, all maps except possibly one are topologically (and even quasiconformally) conjugate; the exception is the center of a hyperbolic component.

A long-standing conjecture is that there are no queer components in the Mandelbrot set—in other words, all components of the interior are hyperbolic. This conjecture is equivalent to the local connectivity of the Mandelbrot set [Douady and Hubbard 1985]. Yoccoz has shown that local connectivity holds for a "substantial" part of Mandelbrot set [Hubbard 1993]. The hyperbolicity conjecture has also been established along the real line by rather different techniques [Świątek 1992; McMullen 1994; Lyubich 1993].

The situation when $\alpha \neq 1$ is quite different, as one should expect, because the iterates of the maps are not uniformly quasiconformal. Douady and Hubbard's proof that the Mandelbrot set is connected relies on the conformal structure; we see no way to adapt it to the nonconformal case. Furthermore, there is no mathematical relationship between the hyperbolicity conjecture and the local connectivity in this case. However, numerical evidence strongly suggests the following conjecture:

Conjecture 5.1. *For all $\alpha > \frac{1}{2}$, the connectedness locus $\mathcal{C}_\alpha$ is connected. However, $\mathcal{C}_\alpha$ is not locally connected for $\alpha \neq 1$.*

The apparent lack of local connectivity of $\mathcal{C}_\alpha$ in the nonconformal case is at least partially related to

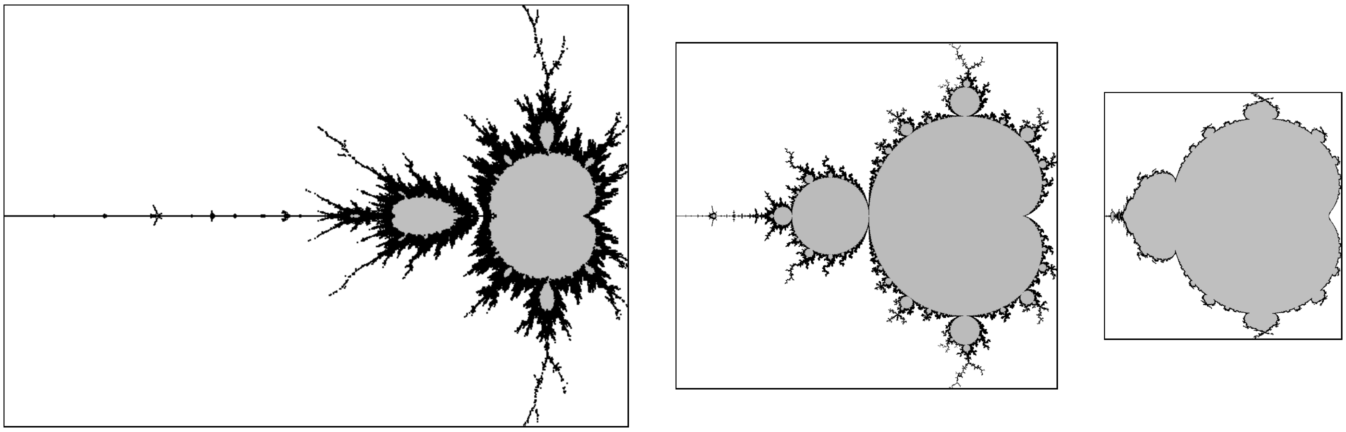

FIGURE 13. The connectedness locus for $\alpha = 0.75$ ($c \in \lfloor -4-1.6i,\ 0.56+1.6i \rceil$), $\alpha = 1$ ($c \in \lfloor -2-1.2i,\ 0.6+1.2i \rceil$), and $\alpha = 1.5$ ($c \in \lfloor -1.45 - i,\ 0.5 + i \rceil$).

the presence of saddle points and their stable and unstable manifolds. Such invariant saddles make a qualitative understanding of the dynamics difficult and a quantitative understanding nearly impossible. In particular, when $\alpha < 1$, one can readily see the difficulty caused by the saddles.

Specifically, consider the interval of real parameters for which the restriction of $f_{\alpha,c}$ to the real line has an attracting (in $\mathbb{R}$) fixed point that attracts the critical point. For some interval of parameters, this fixed point is not an attracting fixed point on $\mathbb{C}$, but is repelling in the imaginary direction (for example, in the region ∘+ discussed in Section 4). Denote this fixed point by z_c and consider its global stable manifold $W^s(z_c)$. Because the dynamics is noninvertible, this global stable manifold is topologically more complicated than for a diffeomorphism. The critical point is in this stable manifold and one might hope that the filled-in Julia set is the closure of this stable manifold. Now consider a parameter value c' which is nearby, but not real. Consider the corresponding fixed point $z_{c'}$ and the corresponding global stable manifold. The critical point is not necessarily contained in this global stable manifold. In fact, the global stable manifold changes with the parameter; sometimes the critical point escapes to infinity and sometimes it is in $W^s(z_c')$. The detailed structure of the connectedness locus is unclear, but it has the topological appearance of a stable manifold. The rough structure of the $\mathcal{C}_\alpha$ for these parameters is that the main lobe (which contains those values of the c for which there is an attracting fixed point) is connected to the period two lobe, (containing those values for which there is an attracting cycle of period two) are connected only by a segment in the real line. A very complicated comb-like structure limits on part of this segment. See Figure 14 (left).

When $\alpha > 1$, there is also an apparent lack of local connectivity near the real line, but in a dynamically different part of $\mathcal{C}_\alpha$—for example, between the limit of period doubling and the creation of an orbit of period 5: see Figure 14 (right). At this time, we have no real understanding of what causes this.

Some insight into the topology of the boundary of the main lobe of $\mathcal{C}_\alpha$ can be gained by looking again at the Hopf bifurcation near the conformal case. We shall analyze the type of bifurcations that

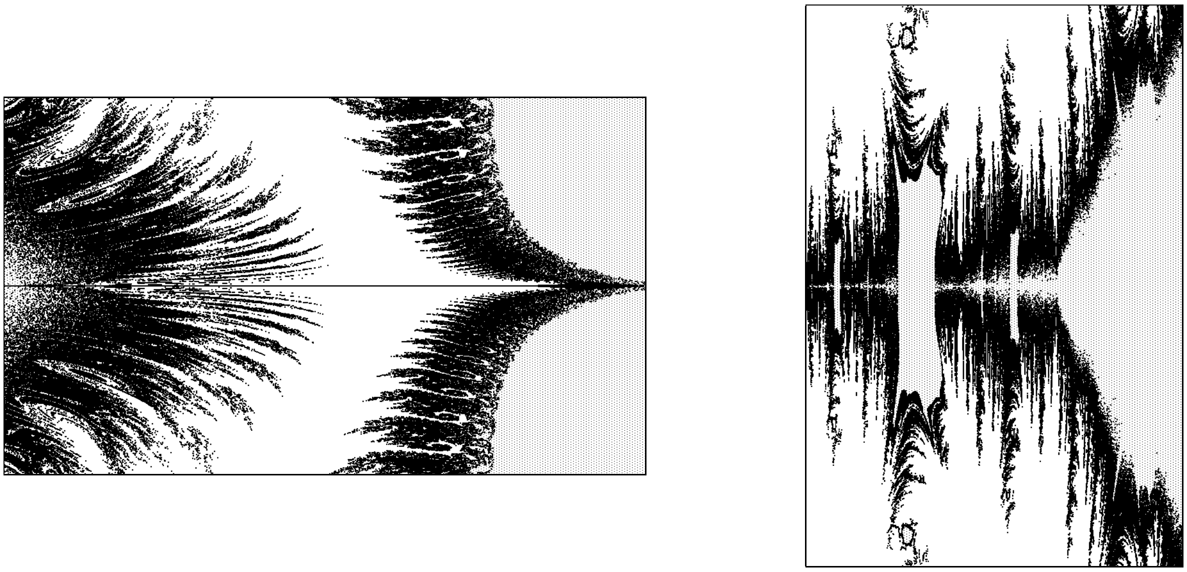

FIGURE 14. Blowups of the connectedness locus for $\alpha = 0.75$ ($c \in \lfloor -0.735-0.09i,\ -0.428+0.09i \rceil$) and $\alpha = 1.5$ ($c \in \lfloor -1.32 - 0.055i, -1.246 + 0.055i \rceil$), showing the apparent lack of local connectivity.

occur near parameters for which there is a fixed point of multiplier λ, where λ is a q-th root of unity, for $q \geq 5$. We shall omit most of the tedious calculations here; the interested reader should refer to [Bielefeld et al. 1991, § 5].

In this situation, one can change coordinates [Marsden and McCracken 1976] so that we have a two complex-parameter family of maps defined near the origin in the complex plane:

$$F_{\mu,a}(z) = \lambda z(e^{\mu} + a|z|^2 + z^q) + O(|az^4|, |a\mu z^3|, |\mu z^{q+1}|, |z^{q+2}|).$$

(Here $a \sim (1-\alpha)/\lambda$.) We are interested in the q-periodic points of $F_{\mu,a}$; one easily sees that for such a point we have

$$z = z(e^{q\mu} + qa|z|^2 + qz^q) + O(|az^4|, |a\mu z^3|, |\mu z^{q+1}|, |z^{q+2}|).$$

We first consider the parameter a to be real, negative, small and fixed. (This corresponds to $\alpha > 1$.) When $\operatorname{Re}\mu \leq 0$, the fixed point $z = 0$ is an attractor; the product of its eigenvalues is less than 1. When $\operatorname{Re}\mu > 0$, the fixed point is repelling, but for $\operatorname{Re}\mu$ sufficiently small, there exists an attracting, invariant (Hopf) circle whose diameter is of order $\sqrt{\operatorname{Re}\mu/|a|}$. One can show that there is also a q-periodic orbit located approximately on the circle of radius $|a|^{1/q-2}$. When $|\mu|$ is small, it is easily seen that this orbit is repelling.

In a horn-shaped domain in the μ-plane, the rotation number on the invariant circle is p/q (recall that $\lambda = e^{2\pi i p/q}$); this horn is in fact the p/q-resonance horn or Arnol'd tongue [Arnol'd 1965; Aronson et al. 1982; Hall 1984]. Within this horn, there are two additional q-periodic orbits: one is a saddle and the other is an attractor; the invariant circle around the repelling fixed point is the closure of the unstable manifold of the p/q-saddle, which contains the attracting orbit. If μ leaves the horn "through the side", i.e., if we fix $\operatorname{Re}\mu$ and vary $\operatorname{Im}\mu$, the saddle and the attractor collide, and although there is still an invariant circle, the rotation number is no longer $\arg\lambda$. If instead we allow $\operatorname{Re}\mu$ to increase sufficiently, the saddle and the repeller collide, leaving a single attracting orbit of period q. However, before this collision occurs, the invariant circle looses smoothness and becomes only a topological circle. This loss of smoothness occurs when the eigenvalues of the p/q-sink become complex. See [Aronson et al. 1982, § 8].

Experimental evidence indicates that the critical orbit remains bounded for all parameter values discussed above: it is attracted to either the attracting fixed point ($\operatorname{Re}\mu < 0$), the invariant circle, or the p/q-periodic attractor. This gives some explanation for the appearance of the connectedness locus near the main lobe: the p/q-lobe sits at the end of a resonance horn, and is hence attached along an arc of values. See Figure 15.

When a is positive (corresponding to $\alpha < 1$), the picture is the other way around. As above, the

FIGURE 15. The $\frac{2}{5}$ limb for $\alpha = 1.5$, in the rectangle $\lfloor -0.6472+0.5856i,\ -0.5031+0.7485i \rceil$. The regions in gray indicate that the critical point converged to a periodic attractor of moderate period (less than 100) within a few hundred iterations. Note the gray horn-like region at the base. The boundary of the figure appears disconnected due to the algorithm used to produce the picture; a different algorithm gives a much thicker boundary.

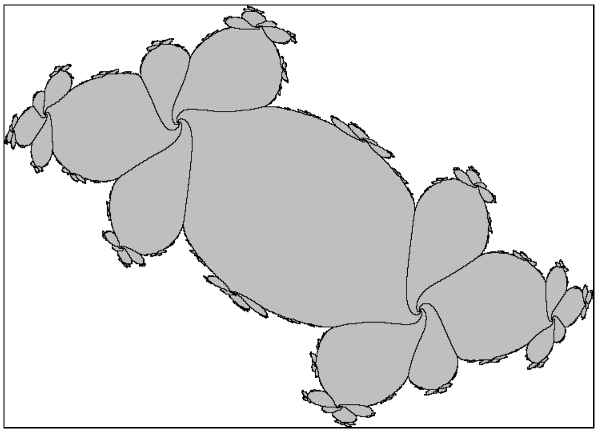

FIGURE 16. A Julia set for c in the $\frac{2}{5}$ resonance horn for $\alpha = 1.5$, $z \in \lfloor -1.25 - 0.9i,\ 1.25 + 0.9i \rceil$. The large gray areas form the basin of the $\frac{2}{5}$ attracting periodic orbit. This attracting orbit has complex eigenvalues, so the unstable manifold of the $\frac{2}{5}$ periodic saddle does not form a smooth invariant circle. This saddle orbit lies on the five smooth curves that divide the gray regions, and that form the stable manifold of the saddle.

fixed point is attracting for $\operatorname{Re}\mu < 0$ and repelling for $\operatorname{Re}\mu > 0$, but the invariant circle is repelling and exists only when $\operatorname{Re}\mu < 0$. Within a horn of μ values, the invariant circle contains a p/q-saddle and a p/q repeller, and is the closure of the stable manifold of the saddle. For all $\operatorname{Re}\mu$ negative and μ sufficiently small, there is another q-periodic orbit nearby, which is attracting.

However, in this case the relationship between the Arnol'd tongue and the connectedness locus is quite different. Since the circle is repelling, for many parameter values in the horn, the critical orbit does not limit on the attracting fixed point; it can escape to ∞, and hence the filled-in Julia set will be disconnected. Thus, one cannot readily detect the presence of the Arnol'd tongues from the connectedness locus alone, as in the case of $\alpha > 1$.

There is, however, a horn-like structure which is readily apparent along the boundary of $\mathcal{C}_\alpha$. See Figure 17. This is related to the presence of q-

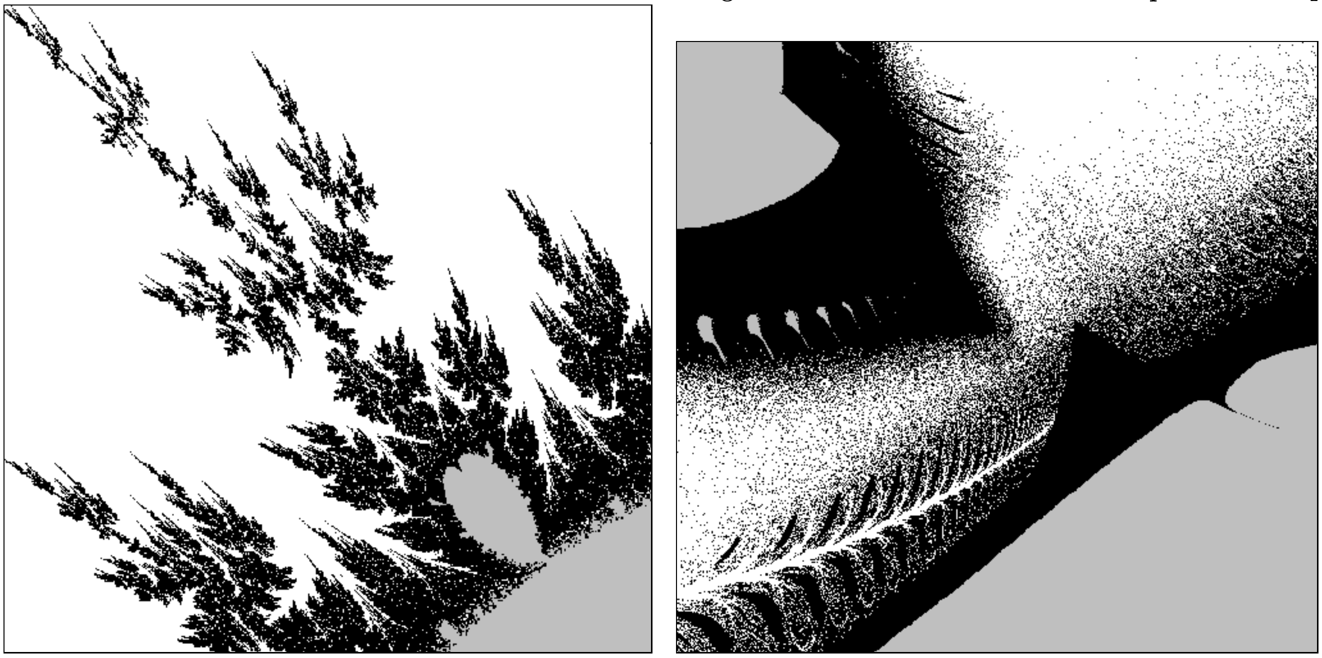

FIGURE 17. Left: the $\frac{2}{5}$ limb for $\alpha = 0.75$, $c \in \lfloor -0.707 + 0.309i,\ -0.265 + 0.721i \rceil$. Right: a blowup with $c \in \lfloor 0.351 + 0.36i,\ -0.324 + 0.386i \rceil$. The two figures were produced with different algorithms; on the left, gray denotes parameters for which the critical point failed to escape within 256 iterations, while on the right such parameter values are colored black, and gray is used to indicate convergence of 0 to an attracting orbit of moderate period.

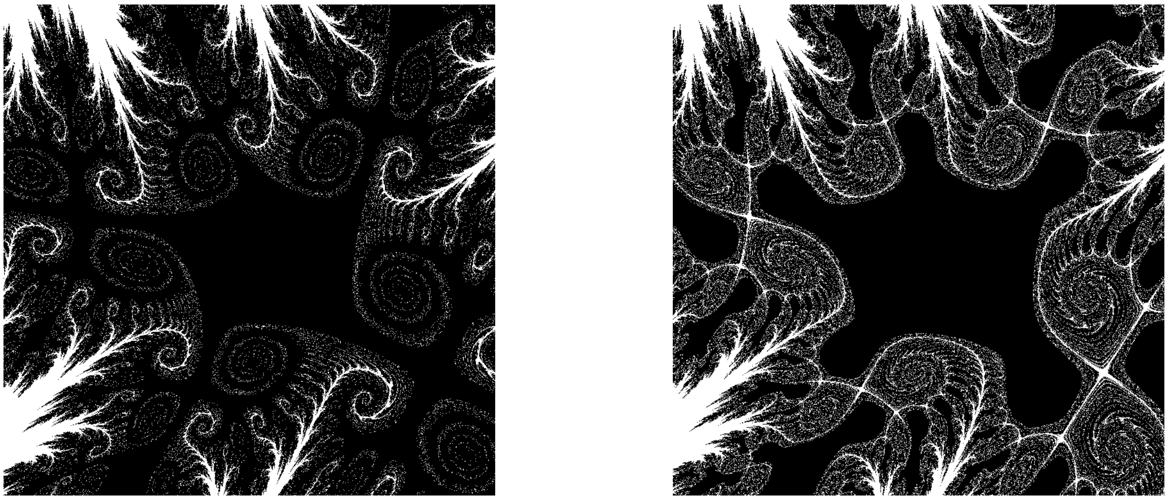

FIGURE 18. Close-ups of the filled Julia set for $\alpha = 0.75$ and $c = -0.333 + 0.372i$, which is within the horn of Figure 17, and for $c = -0.336755 + 0.368516i$, which is just outside the horn. In both cases, $z \in \lfloor -0.7 - 0.2i,\, 0.1 + 0.6i \rceil$ and there is an attracting fixed point at the center of the picture, with a pair of period-five repellers surrounding it (at the ends of the black and white spirals nearest the center on the left figure), and a period-five saddle at the edge of the large black region. On the left, the critical point, 0, lies in the large black cross-shaped region near the lower right. On the right, however, 0 does not lie in the basin of the attractor; it iterates to infinity, and the filled Julia set is disconnected, although not totally disconnected. Notice also that one of the period-five repellers lies in the interior of the filled Julia set.

periodic saddles. Near this horn, there are three period-q orbits, as well as the attracting fixed point. Two of the periodic orbits are repelling, and the the other is a saddle. The horn corresponds to the parameter values for which the critical point lies between the one side of the stable manifold of a saddle point z and the other side of the stable manifold for its image $f_c(z)$. See Figure 18 (left). At the point of the horn, a saddle connection occurs: one side of the local stable manifold of the periodic saddle z is the local unstable manifold for its image $f_c(z)$.

Attached to the top of the horn is a curve for which the critical orbit remains bounded, although it is not attracted to an attractor. For these parameters, the critical point lies on the stable manifold of one of the points of the period-q saddle orbit discussed above. This orbit appears to persist long enough to attach the period-q lobe (within which there is an attracting orbit of period q) to the main lobe. Thus, $\mathcal{C}_\alpha$ is not disconnected as it appears in Figure 17.

ACKNOWLEDGEMENTS

Most of the research for this paper was performed while we were at the Institute for Mathematical Sciences, State University of New York at Stony Brook. We are grateful to the IMS for its support.

REFERENCES

[Ahlfors 1966] L. Ahlfors, *Lectures on Quasiconformal Mappings*, Van Nostrand, Princeton, NJ, 1966 (reprinted by Wadsworth, Monterey, CA, 1987).

[Aronson et al. 1982] D. Aronson, M. Chory, G. R. Hall, R. McGehee, "Bifurcations from an invariant circle for two-parameter families of maps of the plane, a computer-assisted study", *Comm. Math. Phys.* **83** (1982), 303–354.

[Arnol'd 1965] V. I. Arnol'd, "Small denominators I. On the mappings of the circumference of the circle onto itself", *Translations Am. Math. Soc.*, **46** (1965), 213–284.

[Bielefeld et al. 1991] B. Bielefeld, S. Sutherland, F. Tangerman, and J. J. P. Veerman, "Dynamics of certain non-conformal degree two maps of the plane", SUNY Stony Brook IMS preprint 1991/18.

[Blanchard 1984] P. Blanchard, "Complex analytic dynamics on the Riemann sphere", *Bull. Amer. Math. Soc.* **11** (1984), 85–141.

[Devaney 1989] R. Devaney, *An Introduction to Chaotic Dynamical Systems*, 2nd ed., Addison-Wesley, Reading, MA, 1989.

[Douady and Hubbard 1985] A. Douady, and J. Hubbard, "Étude dynamique des polynômes complexes I, II", Publ. Math. d'Orsay 84–02 (1984) and 85–04 (1985).

[Hall 1984] G. R. Hall, "Resonance zones in two-parameter families of circle homeomorphisms", *SIAM J. Math. Anal.* **15** (1984), 1075–1081.

[Hirsch et al. 1977] M. Hirsch, C. Pugh, and M. Shub, *Invariant Manifolds,* Lecture Notes in Mathematics **583**, Springer, New York, 1977.

[Hubbard 1993] J. H. Hubbard, "Local connectivity of Julia sets and bifurcation loci: Three theorems of J.-C. Yoccoz", pp. 467–511 in *Topological Methods in Modern Mathematics, A Symposium in Honor of John Milnor's Sixtieth Birthday*, Publish or Perish, 1993.

[Jiang 1990] Y. Jiang, "Generalized Ulam–von Neumann Transformations", Thesis, City University, New York, 1990.

[Jiang 1993] Y. Jiang, "Dynamics of certain nonconformal semigroups", *Complex Variables* **22** (1993), 27–34.

[Lehto 1987] O. Lehto, *Univalent Functions and Teichmüller Spaces*, Springer, New York, 1987.

[Lyubich 1993] M. Lyubich, "Geometry of quadratic polynomials, moduli, rigidity and local connectivity", SUNY Stony Brook IMS preprint 1993/9.

[McMullen 1994] C. McMullen, *Complex Dynamics and Renormalization*, Princeton University Press, Princeton, NJ, 1994.

[Mañé et al. 1983] R. Mañé, P. Sad, and D. Sullivan, "On the dynamics of rational maps", *Ann. Sci. Éc. Norm. Sup.* (Paris) **16** (1983), 193–217.

[Marsden and McCracken 1976] J. Marsden and M. McCracken, *The Hopf Bifurcation and Its Applications.* Springer, New York, 1976.

[Milnor 1990] J. Milnor, "Dynamics in one complex variable: introductory lectures", SUNY Stony Brook IMS preprint 1990/5.

[Świątek 1992] G. Świątek, "Hyperbolicity is dense in the real quadratic family", SUNY Stony Brook IMS preprint 1992/10.

[Wolfram 1988] S. Wolfram, *Mathematica: A System for Doing Mathematics by Computer*, 2nd ed., Addison-Wesley, Reading, MA, 1991.

Ben Bielefeld, Mathematics Department, National Security Agency, Ft. George G. Meade, MD 20755

Scott Sutherland, Institute for Mathematical Sciences, State University of New York at Stony Brook, Stony Brook, NY 11794-3660 (scott@math.sunysb.edu)

Folkert Tangerman, Center for Advanced Manufacturing, Department of Applied Mathematics and Statistics, State University of New York at Stony Brook, Stony Brook, NY 11794 (tangerma@ams.sunysb.edu)

J. J. P. Veerman, Departamento de Matemática, Universidade Federal de Pernambuco, Cidade Universitária, Rua Prof. Luis Freire, Recife, PE 50740-540, Brazil (veerman@dmat.ufpe.br)

Received January 8, 1992; accepted in revised form March 1, 1994